Accelerated Cellular Senescence in Progressive Multiple Sclerosis: A Histopathological Study

Dimitrios Papadopoulos, MD, PhD,[1,2,3] Roberta Magliozzi, PhD,[4,5] Sara Bandiera, PhD,[5] Ilaria Cimignolo, MSc,[4] Elena Barusolo, MSc,[4] Lesley Probert, PhD,[2] Vassilis Gorgoulis, MD, PhD,[3,6,7] Richard Reynolds, PhD,[5] and Richard Nicholas, FRCP, PhD[5]

Objective: The neurodegenerative processes driving the build-up of disability in progressive multiple sclerosis (P-MS) have not been fully elucidated. Recent data link cellular senescence (CS) to neurodegeneration. We investigated for evidence of CS in P-MS and sought to determine its pattern.

Methods: We used 53BP1, p16, and lipofuscin as markers of CS in white matter lesions (WMLs), normal appearing white matter (NAWM), normal appearing cortical gray matter (NAGM), control white matter (CWM), and control gray matter (CGM) on autopsy material from patient with P-MS and healthy controls. Senescence-associated secretory phenotype (SASP) factors were quantified in cerebrospinal fluid (CSF).

Results: P16$^+$ cell counts were significantly increased in WMLs and GMLs, compared with NAWM, CWM, NAGM, and CGM and lipofuscin$^+$ cells were significantly increased in WMLs, compared with NAWM and CWM, indicating more abundant CS in demyelinated lesions. The 53BP1$^+$ cells in WMLs were significantly increased compared with NAWM and CWM. The 53BP1$^+$ and p16$^+$ cells were found significantly more abundant in acute active WMLs and GMLs, compared with chronic inactive lesions. Co-localization studies showed evidence of CS in neurons, astrocytes, oligodendrocytes, microglia, and macrophages. Among the quantified CSF SASP factors, IL-6, MIF, and MIP1a levels correlated with 53BP1$^+$ cell counts in NAGM, whereas IL-10 levels correlated with p16$^+$ cell counts in NAWM. P16$^+$ cell counts in WMLs exhibited an inverse correlation with time to requiring a wheelchair and with age at death.

Interpretation: Our data indicates that CS primarily affects actively demyelinating gray and WMLs. A higher senescent cell load in P-MS is associated with faster disability progression and death.

ANN NEUROL 2025;97:1074–1087

Age is the most important risk factor for the transition from relapsing multiple sclerosis (R-MS) to secondary-progressive MS (SP-MS).[1] Primary progressive MS (PP-MS) does not occur in pediatric cases and it typically presents at an older age than R-MS.[2] Notably, the older the age the presentation of R-MS the greater the likelihood for transition to SP-MS.[1,3] This association of disability progression with aging has implicated

View this article online at wileyonlinelibrary.com. DOI: 10.1002/ana.27195

Received Aug 15, 2024, and in revised form Dec 29, 2024. Accepted for publication Jan 16, 2025.

Address correspondence to Dr Dimitrios Papadopoulos, School of Medicine, European University Cyprus, 6 Diogenes Street, Engomi, Nicosia, 2404, Cyprus. E-mail: d.papadopoulos@euc.ac.cy

From the [1]School of Medicine, European University, Nicosia, Cyprus; [2]Laboratory of Molecular Genetics, Hellenic Pasteur Institute, Athens, Greece; [3]Molecular Carcinogenesis Group, Department of Histology and Embryology, Faculty of Medicine, National and Kapodistrian University of Athens, Athens, Greece; [4]Department of Neurosciences and Biomedicine and Movement, The Multiple Sclerosis Center of University Hospital of Verona, Verona, Italy; [5]Department of Brain Sciences, Faculty of Medicine, Imperial College London, London, UK; [6]Ninewells Hospital and Medical School, University of Dundee, Dundee, UK; and [7]Division of Cancer Sciences, School of Medical Sciences, Faculty of Biology, Medicine and Health, University of Manchester, Manchester, UK

Additional supporting information can be found in the online version of this article.

 © 2025 The Author(s). *Annals of Neurology* published by Wiley Periodicals LLC on behalf of American Neurological Association.
This is an open access article under the terms of the Creative Commons Attribution-NonCommercial License, which permits use, distribution and reproduction in any medium, provided the original work is properly cited and is not used for commercial purposes.

age-related neurodegenerative processes as pathological substrates of progressive disability worsening.[4,5] Nevertheless, these age-related processes have not yet been clearly identified.

Cellular senescence (CS) is a precisely regulated key cellular process underlying the biological changes of aging[6] with certain features that render it a putative mechanism driving the build-up of disability in progressive MS (P-MS).[7] CS is known to be triggered by a plethora of stressors, including factors common to MS pathology, such as oxidative stress, cytokines and mitochondrial dysfunction, telomere attrition, and replicative stress associated with aging.[8–10] It is characterized by irreversible cell-cycle arrest coupled to stereotypic phenotype changes,[11] which involve morphological alterations, metabolic changes, mitochondrial dysfunction, and changes in the secretome of senescent cells with the secretion of proinflammatory cytokines, matrix metalloproteinases, and other inflammatory mediators, termed senescence-associated secretory phenotype (SASP).[12]

An increasing senescent cell tissue load is thought to culminate in tissues acquiring a pro-inflammatory milieu and losing their normal function and reparative capacities as the extensive changes in gene expression found in senescent cells indicate significant alteration of physiological cell function.[13] All central nervous system (CNS) cell types have been shown to commit to senescence under specific circumstances.[14] Although the strict definition of CS applies to dividing cells arrested at G1/S transition, post-mitotic cells like neurons may also attain a senescence-like phenotype and may even upregulate cell-cycle regulators, such as p16 and p21, as several stressors and neurodegenerative disease conditions have been shown to induce an abortive unscheduled cell cycle in post-mitotic neurons.[15–17] Evidence indicates that senescent cells can convert neighboring cells to senescence by exerting a bystander effect mediated by the paracrine action of pro-inflammatory mediators.[18,19] In addition, senescent cells may also accumulate over time under conditions of persistent tissue damage or in aged tissues where their immune-mediated clearance fails.[20,21] Despite the initial consideration of cell senescence as a homeostatic response aiming to prevent proliferation of damaged cells, it is now thought to contribute to loss of function associated with aging and age-related neurodegenerative diseases.[22] The elimination of senescent cells using pharmacological or genetic manipulations has been shown to prevent neurodegenerative changes and cognitive deficits in murine genetic models of amyloid-β and τ-mediated neurodegeneration.[23,24] We have previously provided evidence of senescent glial cells in acute, chronic active, and chronic inactive demyelinated white matter MS lesions.[14] Senescent cell accumulation in MS may be at least partly responsible for the age-related neurodegeneration thought to be driving disability progression in MS.[25]

The aim of this study was to test the hypothesis that there is accelerated CS of neurons and glial cells in P-MS, by performing a quantitative histopathological analysis of senescence markers in autopsy material. We sought to explore which cell types may be more susceptible to becoming senescent and if there is any predilection of CS for lesion stages and topographic patterns. Furthermore, we examined if CS is associated with key features of MS pathology, such as inflammation and astrogliosis and clinical milestones of disease severity. Given that no marker is entirely specific for CS we have followed the International Cell Senescence Association (ICSA) consensus recommendations and have combined 3 different markers.[12]

Materials and Methods

Tissue Samples

MS and control formalin-fixed, paraffin-embedded, and fixed-frozen tissue blocks were obtained from the UK Multiple Sclerosis Tissue Bank at Imperial College London. All MS tissue blocks were chosen to contain a subcortical or juxtacortical white matter demyelinating lesion (WML) along with the adjacent normal appearing white matter (NAWM) and normal appearing cortical gray matter (NAGM) or gray matter demyelinating lesions (GMLs). Control tissue blocks contained subcortical/juxtacortical white matter (CWM) and adjacent cortical gray matter (CGM). Fully informed consent for all the tissue and clinical information was obtained, via a prospective donor scheme, with approval from the Multicentre Research Ethics Committee (MREC/02/2/39).

One to 2 blocks per case from a total of 44 cases were included in the study; 30 progressive MS cases and 14 controls. The MS cases (21 female patients and 9 male patients) were neuropathologically confirmed. Ten healthy cases (4 female patients and 6 male patients) were used as controls. The clinical and neuropathological examination reports provided by the MS tissue bank were used to exclude all cases with a history of chemotherapy or radiotherapy and findings suggestive of other neurodegenerative or metastatic disease. All relevant demographic and clinical data of the cases analyzed are presented in Supplementary Table S1.

Histochemistry, Immunohistochemistry, and Immunofluorescence Staining

Seven μm thick serial sections from paraffin-embedded tissue blocks were stained with hematoxylin and eosin (H&E), Luxol-fast blue and cresyl fast violet (LFB/CFV). Immunohistochemistry for MOG, HLA class II (DAKO), GFAP (DAKO), GAD67 (Abcam), NFil-High MW (Santa Cruz), Olig-2 (Millipore), Iba-1 (WAKO), TMEM-119 (Atlas, Bromma), MAP-2 (Thermo Fisher), $p16^{INK4A}$ (Abcam), and 53BP1 (Novus) were

performed with the standard avidin-biotin-horseradish peroxidase method (Vectastain ABC Elite, Vector Labs, UK). Lipofuscin was detected with the GL13 hybrid histochemistry-immunohistochemistry method (SENTRAGOR), according to the manufacturer's standard protocol.[26] Sections were counter-stained with hematoxylin. The egative controls included IgG isotype controls or pre-immune serum, or omission of the primary antibody or GL13 stain.

MOG, HLA class II, GFAP, 53BP1, p16, and GL13-stained sections were captured with an Axiocam 208 Colorcamera fitted to an Axioscope microscope (ZEISS International, Germany). All captured images were coded and analyzed in a blinded manner. Identification of ectopic lymphoid follicle-like structures was performed as previously described.[27]

Double immunofluorescence staining was performed to co-localize 53BP1, p16, and GL13/lipofuscin staining with each other and with cell-specific markers on paraformaldehyde-fixed frozen sections according to standard protocols. Cy3-, rhodamine-, or fluorescein-conjugated anti-rabbit and anti-goat IgG and fluorescein- or rhodamine-conjugated anti-mouse IgG were used as secondary antibodies. For negative controls, the primary antibodies were replaced with preimmune serum or IgG isotype controls.

Staging of Multiple Sclerosis Lesions

White matter and cortical demyelinated lesions were staged as acute active (AA), chronic active (CA), or chronic inactive (CI) according to previously published staging criteria using myelin oligodendrocyte glycoprotein (MOG), HLA class II (microglia/macrophages), and CD3 (T lymphocytes) immunohistochemistry.[27,28] Leukocortical lesions were classified as AA, CA, and CI according to the distribution and density of HLA class II^+ cells in their white matter parts.[29] Intracortical and subpial cortical lesions were staged based on the density and distribution of HLA class II^+ cells with active cortical lesions having a distinct border of HLA class II^+ cells, located at the cortical lesion edge, and cores with increased HLA class II^+ cell density compared to a healthy cortex. Chronic active cortical lesions had a border of HLA class II^+ cells and decreased or normal densities of HLA class II^+ cells in their cores when compared to normal cortex. Chronic inactive cortical lesions had no clear border of HLA class II^+ cells but had cores with densities of HLA class II^+ cells similar to a healthy appearing cortex.[29]

Quantification of Demyelination, Inflammatory Infiltration, and Astrogliosis

The size of WMLs and GMLs was quantified on one section from each paraformaldehyde-fixed tissue block immunostained for MOG. Digital images were captured at 0.5 × magnification. The areas of demyelination and the total area of WM and GM were manually outlined for each section. Quantification was performed in WMLs, NAWM, NAGM, and control subcortical/juxtacortical WM and CGM. The area covered by HLA class II immunoreactivity was measured on images from 3 sections per block, by counting the number of pixels above a set threshold. Images were converted to grey scale 8 bpp. Signal intensity segmentation thresholds were defined to optimize accuracy and reproducibility. Vessels and artifacts were manually excluded. HLA class II immunoreactivity was expressed as a percentage of the sampled area covered by HLA class II immunostaining. GFAP immunostained cells were measured on images from 3 sections per block using Image Pro-Plus version 6.0 software.

Quantification of 53BP1 Immunoreactivity and GL13/Lipofuscin Staining

Immunohistochemistry for 53BP1 (a marker of DNA damage response-DDR) and GL13 staining were performed on 7 μm thick sections. Quantification was performed in WMLs, NAWM, NAGM, and control subcortical/juxtacortical WM and CGM. The 53BP1 and GL13-stained cells were counted in WMLs and expressed as a percentage of the total number of cells per WMLs. The 53BP1 and GL13 counts were performed on images from 3 sections per block using Image Pro-Plus version 6.0 software.

Quantification of SASP Markers in Post-Mortem CSF

The levels of several SASP factors (EOTAXIN-3/CCL26, Gro-alpha/CXCL1, Gro-Beta/CXCL2, MCP-1/CCL2, MCP-3/CCL7, MIF, MIG/CXCL9, MIP-1alpha/CCL3, MIP-3alpha/CCL20, TECK/ CCL25, TNF-α, IL-6, IL-8/CXCL8, IL-10, IL-22, IL-27(p28), IL-32)[30,31] were determined in the cerebrospinal fluid (CSF) samples of MS cases and controls using custom immune-assay multiplex Luminex technology (Bio-Plex X200 System equipped with a magnetic workstation; BioRad, Hercules, CA), as previously described.[32] SASP factors were quantified in a subpopulation of 14 MS cases with available CSF marked with an asterisk in Supplementary Table S1 (9 female patients and 5 male patients). A separate group of 10 CSF healthy controls was used (C001–C010, 3 female patients and 7 male patients; see Supplementary Table S1).

Statistical Analysis

Normality of distribution of variables was tested with the D'Agostino and Pearson test. Comparisons of means between the 2 groups were performed with the Student's t test. Thje $53BP1^+$, $p16^+$, and GL-13/lipofuscin$^+$ cell counts in WMLs, GMLs, NAWM, NAGM, and CWM and CGM were compared using 1-way analysis of variance (ANOVA) and pairwise comparisons were performed with Fisher's Least Significant Difference (LSD) post hoc test. Correlation analyses were performed with the Pearson's product moment correlation test. Significance was assessed at $p < 0.05$. All values are reported as mean ± SD unless otherwise stated. PRISM version 9.4 (GraphPad) was used for statistical analysis.

Results

Cellular Senescence is Increased in MS Lesions and in Normal Appearing White and Gray Matter

Despite the mean age of P-MS cases not differing from that of the healthy controls (see Supplementary Table S1),

quantification of p16$^+$, an inducer of G1 stage cell-cycle arrest and a marker of cellular senescence,[33] revealed a significantly greater load of p16$^+$ cells in MS tissues compared with healthy controls. More specifically, a 17.6-fold increase in p16$^+$ cells in WMLs was found compared to CWM ($p < 0.001$) and a 3.95-fold increase compared to NAWM ($p < 0.05$; Fig 1A). A similar pattern was observed in GMLs, with p16$^+$ cells that were found to be increased 8-fold compared to control CGM and 2.92-fold increase compared to NAGM ($p < 0.001$; see Fig 1A). As previously described, the blocks from ectopic lymph follicle-like positive cases (LFL$^+$, n = 11) exhibited significantly more extensive demyelination in the WM (39.3% ± 3.4 demyelinated area) and GM (68.9% ± 9.4 demyelinated GM area), than blocks from cases without ectopic lymph follicle-like structures (25.4% ± 3.2 of WM and 36.2% ± 1.6 of GM areas, LFL$^-$, n = 3, $p < 0.0001$ for both comparisons).[34] No significant difference in p16$^+$ cell counts was observed between LFL$^+$ and LFL$^-$ P-MS cases in the NAWM, NAGM, GMLs, or WMLs (data not shown).

GL-13, a lipofuscin stain was also used as marker of CS, as senescence-associated metabolic deregulation frequently leads to lipofuscin accumulation in senescent cells.[26] In MS cases, GL-13/lipofuscin$^+$ cells were significantly increased in WM lesions 1.5-fold, compared to NAWM and 2.7-fold, compared to CWM ($p < 0.01$, Fig 1B). No statistically significant correlation was observed between the number of GL-13/lipofuscin$^+$ cells and GFAP or HLA class II immunoreactivity in WMLs or NAWM. Given that DNA damage response (DDR) is an upstream event and a common trigger of CS we then sought to quantify DDR in our samples.[21]

Extensive Activation of the DNA Damage Response in Demyelinated White and Gray Matter Lesions in P-MS

The 53BP1 is a crucial component of DNA double-strand break (DSB) signaling and a marker of activated DDR.[35] Quantification of 53BP1$^+$ immunostaining revealed a 22.4-fold increase in the number of 53BP1$^+$ cells in WMLs in patients with P-MS compared with healthy CWM ($p < 0.001$; Fig 1C). The number of 53BP1$^+$ cells was also significantly greater in WMLs, compared to MS NAWM (2.48-fold increase, $p < 0.05$; see Fig 1C). The 53BP1$^+$ cells showed a 9-fold increase in NAWM compared with age-matched control WM ($p < 0.05$).

Similarly, a 50-fold increase in 53BP1$^+$ cells was observed in CGM demyelinated lesions, in comparison to control CGM ($p < 0.001$; see Fig 1C). The number of 53BP1$^+$ cells in GMLs was also found to be 3.9-times higher than in P-MS NAGM ($p < 0.01$; see Fig 1C). A 12.95-fold increase in 53BP1$^+$ cells in NAWM were also significantly increased by 12.9-fold compared to CGM ($p < 0.001$; see Fig 1C).

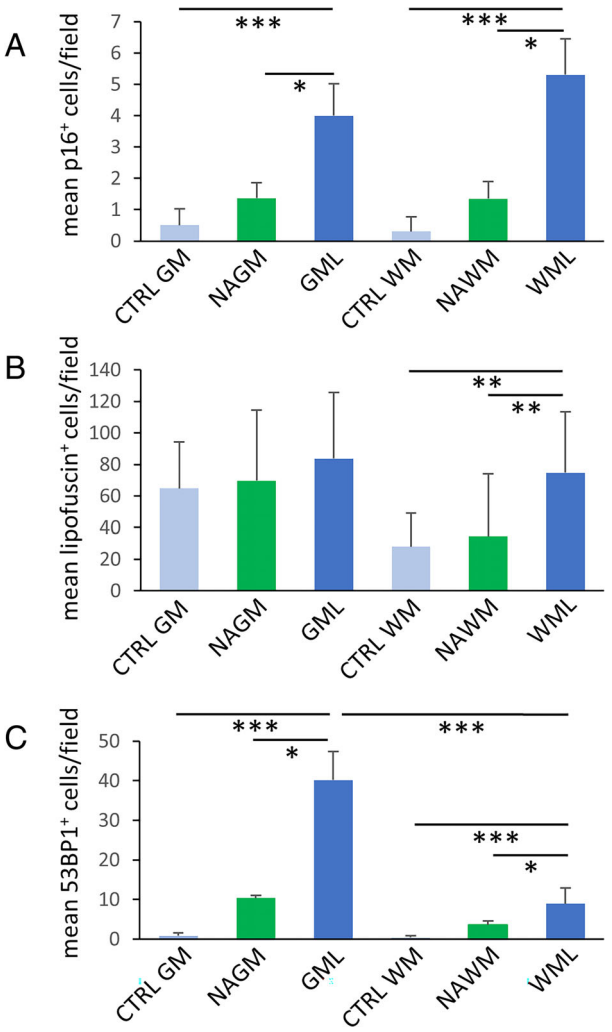

FIGURE 1: Markers of cellular senescence and DDR indicate more extensive cellular senescence in progressive MS compared to controls. (A) Quantification of p16$^+$ cell counts (number of p16$^+$ cells/field). Statistical comparisons performed with one-way ANOVA and Fisher's LSD post hoc test for multiple comparisons. Quantification of GL13$^+$ lipofuscin-containing cells (cells/field). (B) Lipofuscin-containing cells were found significantly increased in WMLs, compared with NAWM (n = 16 blocks from 10 P-MS cases) and (n = 10 blocks from 10 control cases, $p < 0.01$). Statistical testing with 1-way ANOVA and pair-wise comparisons with the Fisher's LSD test. Quantification of 53BP1$^+$ cells (cells/field). (C) The 53BP1$^+$ cells were found significantly increased in WMLs, compared with NAWM (P-MS cases, n = 30) and CTRL WM (CTRLs, n = 10). Similarly, 53BP1$^+$ cells were found significantly increased in GMLs, compared to NAGM and CTRL GM. Statistical testing with one-way ANOVA and pair-wise comparisons with the Fisher's LSD test. Error bars = SD; *$p < 0.05$, ***$p < 0.0001$; ANOVA = analysis of variance; CTRL = control; DDR = DNA damage response; GM = gray matter; GMLs = gray matter demyelinated lesions; LSD = Least Significant Difference; MS = multiple sclerosis; NAGM = normal appearing gray matter; NAWM = normal appearing white matter; WM = white matter; WML = white matter demyelinated lesion. [Color figure can be viewed at www.annalsofneurology.org]

The significantly greater numbers of 53BP1$^+$ cells in WMLs and GMLs compared to NAWM and NAGM, respectively, suggest a link between demyelination and DNA damage response. Furthermore, comparison of 53BP1$^+$ cell counts between P-MS gray and white matter revealed significantly greater numbers of 53BP1$^+$ cells in GMLs compared with WMLs ($p < 0.001$) and in NAGM compared to NAWM ($p < 0.05$), indicating more extensive activation of the DNA damage response pathway in the gray than in the white matter in P-MS (see Fig 1C).

Notably, correlation analysis also revealed a significant association between the number of 53BP1$^+$ cells and p16$^+$ cell counts in WMLs ($r_P = 0.794$, $p < 0.0001$) and NAWM ($r_P = 0.566$, $p = 0.0336$; Fig 2A, B). This association between DDR and p16 activation suggests that CS is largely elicited by DNA damage. Nevertheless, correlation analysis revealed no significant link between the 53BP1$^+$ cell counts and HLA class II immunoreactivity or GFAP immunoreactivity in WMLs, GMLs, NAWM, or NAGM.

Cellular Senescence is Lesion Stage-Dependent, and it is more Extensive in Lesions With Active Inflammatory Demyelination

Out of the 30 white matter demyelinated lesions identified in the 30 blocks examined, 7 were classified as AA, 6 as chronic active CA, and 17 as CI. Similarly, out of the 30 gray matter demyelinated lesions identified in the 30 blocks examined, 9 were classified as AA, 10 were CA, and 11 were CI. The 53BP1$^+$ cell counts were significantly higher in AA lesions (14.0 ± 3.0), compared to CA (10.8 ± 3.6, $p < 0.05$) and CI white matter lesions (WMLs; 6.23 ± 1.0, $p < 0.0001$). CA lesions also exhibited significantly higher 53BP1$^+$ cell counts than CI WMLs ($p < 0.0001$; Fig 3A). Nevertheless, 53BP1$^+$ cell counts in CI WMLs were 15-fold higher than in CWM (0.40 ± 0.51, $p < 0.0001$). A similar pattern was observed with 53BP1$^+$ cell counts in CGM lesions, with AA (44.1 ± 9.9) and CA cortical lesions (42.3 ± 3.9) exhibiting significantly higher 53BP1$^+$ cell counts than CI (35.0 ± 3.0, $p < 0.01$ and $p < 0.05$). The 53BP1$^+$ cell counts in CI GM lesions were 43-fold higher than in control gray matter (0.80 ± 0.78, $p < 0.0001$; see Fig 3A).

Quantification of p16$^+$ cells in white matter demyelinated lesions of different stages revealed significantly higher p16$^+$ cell counts in AA ($p < 0.0001$) and CA lesions ($p < 0.001$), compared to CI WM lesions (Fig 3B). Nevertheless, p16$^+$ cell counts in CI WMLs (4.52 ± 0.51) were 15-fold higher than in the control white matter (CWM; 0.30 ± 0.38, $p < 0.0001$). Gray matter demyelinated lesions exhibited a similar pattern with p16$^+$ cell counts in AA lesions being significantly higher (5.11 ± 0.78) than CA (3.90 ± 0.56, $p < 0.001$) and CI lesions (3.18 ± 0.60, $p < 0.0001$). P16$^+$ cell counts in CI GMLs were 6-fold higher than in CWM (0.50 ± 0.52, $p < 0.0001$; see Fig 3B).

Evidence of DNA Damage Response and Cellular Senescence in Neurons and Glial Cells in Gray and White Matter

Staining for 53BP1 indicated activated DNA damage response in cells of the NAGM, cortical and deep gray matter demyelinated lesions, and NAWM and WMLs. A greater frequency of 53BP1$^+$ cells was observed in the NAGM, compared to the NAWM (Fig 4A). In periventricular gray and WMLs and in CGM, a surface-in spatial gradient of 53BP1 expression was observed with cells exhibiting DDR being more numerous the closer they were to the ependymal lining (Fig 4B) or to the pial-CSF boundary (Fig 4F). Immunostaining for p16 showed a higher frequency of p16$^+$ cells in NAWM, compared to the NAGM areas (Fig 4F, G) and in WMLs, compared to GMLs (Fig 5D). P16 immunoreactivity was also observed in perivascular and meningeal infiltrates (see Fig 4C, D).

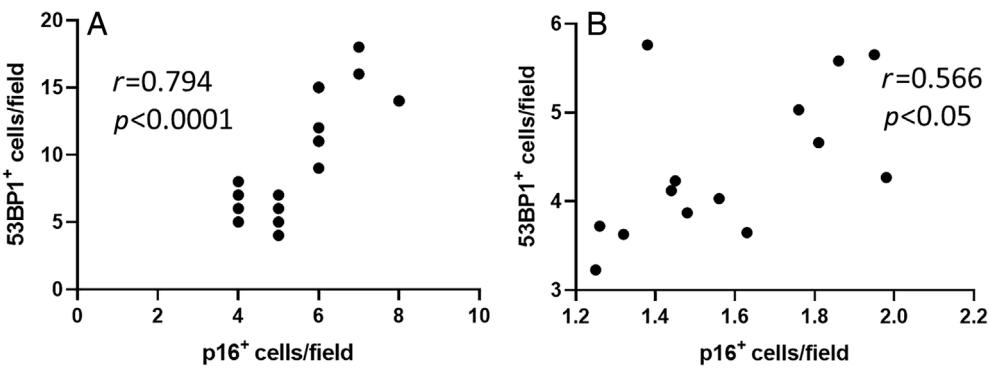

FIGURE 2: Correlation analysis between DDR (53BP1$^+$ cell counts) and CS (p16). (A) Correlation between 53BP1$^+$ cells counts and p16$^+$ cell counts in WMLs (n = 30). (B) Correlation between 53BP1$^+$ cells counts and p16$^+$ cell counts in the NAWM (n = 14). Correlations were tested with the Pearson's correlation coefficient. CS = cellular senescence; DDR = DNA damage response; NAWM = normal-appearing white matter; WML = white matter demyelinated lesion.

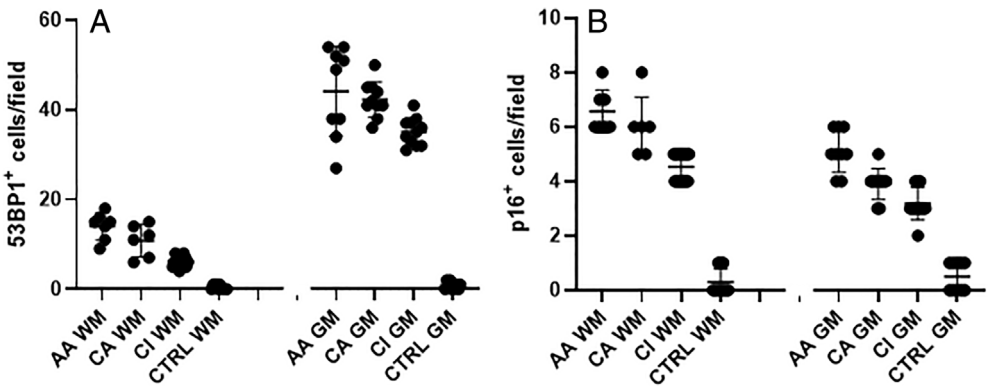

FIGURE 3: The 53BP1$^+$ cell counts (marker of DDR) and p16$^+$ cell counts (marker of CS) according to demyelinating lesion stage. (A) The 53BP1$^+$ cell counts according to WM and GM demyelinated lesion stage. All WM lesion stages differ significantly in 53BP1$^+$ cell counts ($p < 0.001$ for all comparisons except AA WMLs vs CA WMLs $p < 0.05$). All GM lesions differed significantly in 53BP1$^+$ cell counts ($p < 0.001$ for all comparisons except CA WMLs vs CI GMLs $p < 0.05$) but there was no significant difference in 53BP1$^+$ cell counts between AA GM and CA GM lesions. (B) The p16$^+$ cell counts according to WM and GM demyelinated lesion stage. All WM lesions differ significantly in p16$^+$ cell counts ($p < 0.001$ for all comparisons). The p16$^+$ cell counts do not differ significantly between AA WM and CA WM lesions. All GM lesions differ significantly in p16$^+$ cell counts ($p < 0.001$ for all comparisons) except between CA and CI GM lesions ($p > 0.05$). Differences between groups tested with one-way ANOVA separately for WM and GM lesions. Multiple comparisons with Tukey's test. Error bars: mean ± SD. AA = acute active; ANOVA = analysis of variance; CA = chronic active; CI = chronic inactive; CS = cellular senescence; CTRL = controls; DDR = DNA damage response; GM = gray matter; GMLs = gray matter demyelinated lesions; LSD = Least Significant Difference; WM = white matter; WML = white matter demyelinated lesion.

GL13 immunostaining in CA (Fig 6A–C), CA (Fig 6D–F), and CI lesions (Fig 6G–I) revealed lipofuscin accumulation in glial cells, neurons, and perivascular immune cells (Fig 6J–L).

The specificity of the 53BP1 and p16 markers as markers of the senescence pathway was verified using double immunofluorescence with GL13/lipofuscin, confirming the accuracy of these markers in identifying senescent cells (see Fig 4 inset in Fig 4A, D). Quantification of 53BP1$^+$ and p16$^+$ cells showed 41% of cells being 53BP1$^+$ and 36% being p16$^+$ in acute active GMLs (Fig 5C, D). On the contrary, 58.2% of cells were p16$^+$ and 31.5% were 53BP1$^+$ in acute active WMLs (see Fig 5C, D). In AA WMLs, 11% of the cells were found to be 53BP1$^+$/GL13$^+$ and 9% were found to be p16$^+$/GL13$^+$ double positive, whereas in acute GMLs, 36% were found to be 53BP1$^+$/GL13$^+$ and 9% were found to be p16$^+$/GL13$^+$ double positive (see Fig 5C, D).

Most of the p16$^+$ cells were GFAP$^+$ astrocytes (see Fig 4K) and sporadically MAP2$^+$ neurons (see Fig 4K, L). Immunohistochemical double staining for HLA class II with 53BP1 and p16 revealed a frequent pattern of contact between HLA class II$^+$ cells with ramified morphology reminiscent of microglia with 53BP1 and p16$^+$ cells (Fig 4M). Quantification of 53BP1 immunofluorescence co-localizing with different cell-specific markers in cortical demyelinated lesions showed that 40.9% of 53BP1$^+$ cells were MAP-2$^+$ neurons, 33.1% were Olig2$^+$ oligodendrocytes/oligodendrocyte progenitors and 26.0% were GFAP$^+$ astrocytes (see Figs 4I, J and 5A). Quantification of GL13/lipofuscin immunofluorescence co-localizing with different cell-specific markers in cortical demyelinated lesions showed that 21.2% of lipofuscin$^+$ cells were MAP2$^+$ neurons, 20.2% were Olig2$^+$ oligodendrocytes/oligodendrocyte progenitors, and 5.0% were GFAP$^+$ astrocytes, 8.8% were TMEM119$^+$ microglia, and 22.6% were Iba1+ microglia/macrophages (see Fig 5B).

Senescence-Associated Secretory Phenotype Factors Were Found Increased in the CSF of Progressive MS Cases

As the SASP constitutes a hallmark of senescence and an important mediator of its potentially detrimental actions, several SASP factors were quantified in the CSF of a subgroup of our P-MS cases (age = 51.5 ± 10.2, n = 14) and healthy controls (age = 67.9 ± 20.9, n = 10, $p < 0.05$). SASP factors IL-6, IL-10, Gro-β/CXCL2, MCP-3/CCL7, MIP1a/CCL3, TECK/CCL-25, TNF-a, and MIF, were found significantly increased in the CSF of P-MS cases, compared with controls ($p < 0.05$ for all; Fig 7A–H). Eotaxin-3/CCL26, Gro-alpha/CXCL1, MIG/CXCL9, IL-8/CXCL8, IL-22, IL-27(p28), MCP-1/CCL2, MIP3a/CCL20, and IL-32 in the CSF did not differ significantly between P-MS cases and healthy controls. CSF IL-6, MIF, and MIP1a/CCL3 levels correlated with 53BP1$^+$ cell counts in NAGM, ($r_P = 0.637$, $p < 0.001$; $r_P = 0.511$, $p < 0.05$, and $r_P = 0.414$, $p < 0.05$, respectively; Fig 7I–K), whereas IL-10 levels correlated with

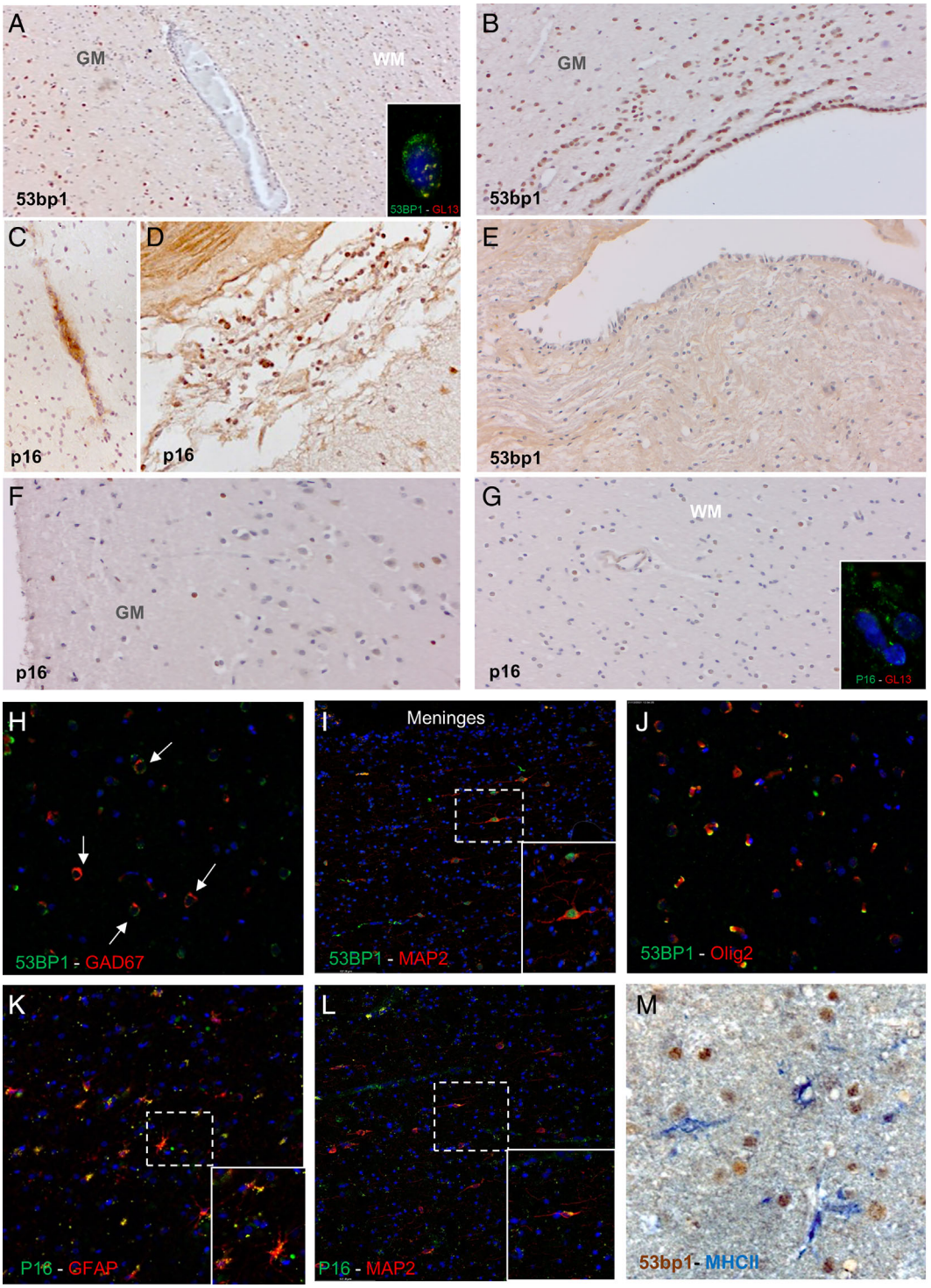

FIGURE 4: Distribution of senescent cells in GMLs and WMLs of progressive MS cases. (A) More 53BP1^{+} senescent cells have been identified in GMLs, compared to WMLs. (B) Abundant 53BP1 immunostaining with a surface-in gradient distribution in a periventricular area also present in ependymal cells in an MS case, but not in a healthy control (E). P16 expression in perivascular (C) and meningeal inflammatory infiltrates (D). More p16^{+} senescent cells have been identified in WMLs (G), compared to GMLs (F). The specificity of these 2 markers as a marker of CS was confirmed using double immunofluorescence with GL13/lipofuscin (*inset* in A and in G). The 53BP1 marker has been identified to be expressed by both GAD67^{+} (H, white arrows) and MAP2^{+} neurons (I), according to a surface-in gradient, more pronounced in areas nearest to the meninges/CSF, as opposed to more distal areas (I). A smaller number of Olig2^{+} oligodendrocytes express 53BP1 (J). The p16 marker, was found highly expressed by GFAP^{+} astrocytes in WMLs (K), and by sporadic MAP^{+} neurons in the GML (L). Activated microglial cells (HLA II^{+} cells) were frequently found close to 53BP1^{+} senescent cells (M). CS = cellular senescence; CSF = cerebrospinal fluid; GMLs = gray matter demyelinated lesions; MS = multiple sclerosis; WMLs = white matter demyelinated lesions. [Color figure can be viewed at www.annalsofneurology.org]

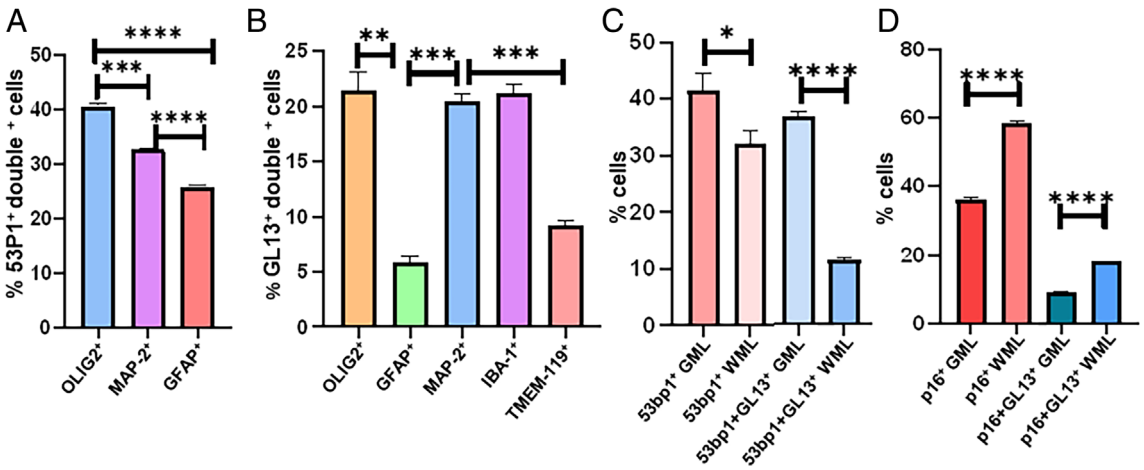

FIGURE 5: Evidence of cellular senescence in astrocytes, oligodendrocytes, neurons, microglia, and macrophages quantified in acute active WMLs and GMLs. (A) Quantification of 51BP1$^+$ cells double-stained with GFAP (astrocytes), Olig-2 (oligodendrocytes/oligodendrocyte progenitor cells), and MAP-2 (interneurons) in cortical demyelinated lesions (GMLs). (B) Percentage of GL-13/lipofuscin$^+$ cells double-immunostained with MAP-2, GFAP, Olig-2, TMEM-119 (microglia), and Iba-1 (microglia/macrophages). (C) Percentage of 53BP1$^+$ and double-immunostained 53BP1$^+$ GL13$^+$ cells in WMLs and GMLs. (D) Percentage of p16$^+$ and double-immunostained p16$^+$GL13$^+$ cells in WMLs and GMLs. Comparisons tested with the Student's *t* test. Error bars = mean ± SD. *$p < 0.05$, **$p < 0.01$, ***$p < 0.001$, ****$p < 0.0001$. GMLs = gray matter demyelinated lesions; WMLs = white matter demyelinated lesions. [Color figure can be viewed at www.annalsofneurology.org]

p16$^+$ cell counts in NAWM ($r_P = 0.62$, $p < 0.01$; Fig 7L).

Increased Senescent Cell Load is Associated With Earlier Disability Progression and Death

Correlation analysis of p16 in WMLs exhibited an inverse correlation with the time from diagnosis to requiring a wheelchair (time to Expanded Disability Status Scale [EDSS] 7.0, $r_P = -0.504$, $p < 0.05$), which indicates that the greater the senescent cell load in WMLs, the faster the disability progression in P-MS (Fig 8A). No significant correlation was observed between and 53BP1 or p16 in GMLs, NAWM, or NAGM and time to requiring a wheelchair (EDSS 7.0). In addition, correlation analysis of p16$^+$ cell counts in NAGM with age at death revealed an inverse correlation ($r_P = -0.45$, $p < 0.05$; Fig 8B). The 53BP1$^+$ cell counts also exhibited an inverse correlation with age at death in WMLs ($r_P = -0.38$, $p < 0.05$; Fig 8C). These findings suggest that the greater the senescent cell load in WMLs and NAWM the greater the disability progression in progressive MS.

Discussion

In recent years, numerous studies have demonstrated that senescent cells become more abundant with aging and that their accumulation may contribute to tissue injury and age-related neurodegeneration.[6,22] This study examined whether there is evidence of accelerated cellular senescence in progressive MS. Our data showed a significantly higher senescent cell load in progressive MS autopsy tissues, compared with age-matched healthy controls. This higher senescent cell load is associated with increased expression of SASP factors in the CSF. Furthermore, the increased senescent cell load was linked to a poorer prognosis with earlier progression to wheelchair and earlier death. The similarity in the pattern of p16, lipofuscin$^+$, and 53BP1$^+$ cell counts, the colocalization studies of DDR and CS markers, and the significant correlation between 53BP1 and p16 cell counts in WMLs and NAWM confirm the internal validity of our findings.

CS is triggered by a multitude of acute and chronic forms of injury to the cell.[36] Our finding of upregulated 53BP1, a marker of DNA damage response correlating with p16 staining in WML, NAWM, and GMLs indicates that CS in progressive MS is largely mediated by irreparable damage to the DNA of resident CNS cells. In addition, the senescent cell load being greatest in acute active lesions suggest that CS in MS lesions may be elicited by inflammation-related DNA damage. Apart from stochastic and environmental insult-related DNA damage that builds up over time and is also seen in age-matched controls, the excess DNA damage seen in progressive MS may be due to the increased levels of oxidative stress particularly affecting neurons and oligodendrocytes in association with active demyelination and neuroaxonal injury.[37] Oxidative damage to nucleic acids, lipids, and proteins is known to be augmented by metals such as iron and zinc.[38,39] A subset of chronic inactive and chronic active lesions that are most frequently found in progressive MS are characterized by iron-enriched cells.[40,41] Nevertheless, damage to the neuronal mitochondria and their DNA[10,42] may also contribute to the high senescent cell load seen in progressive

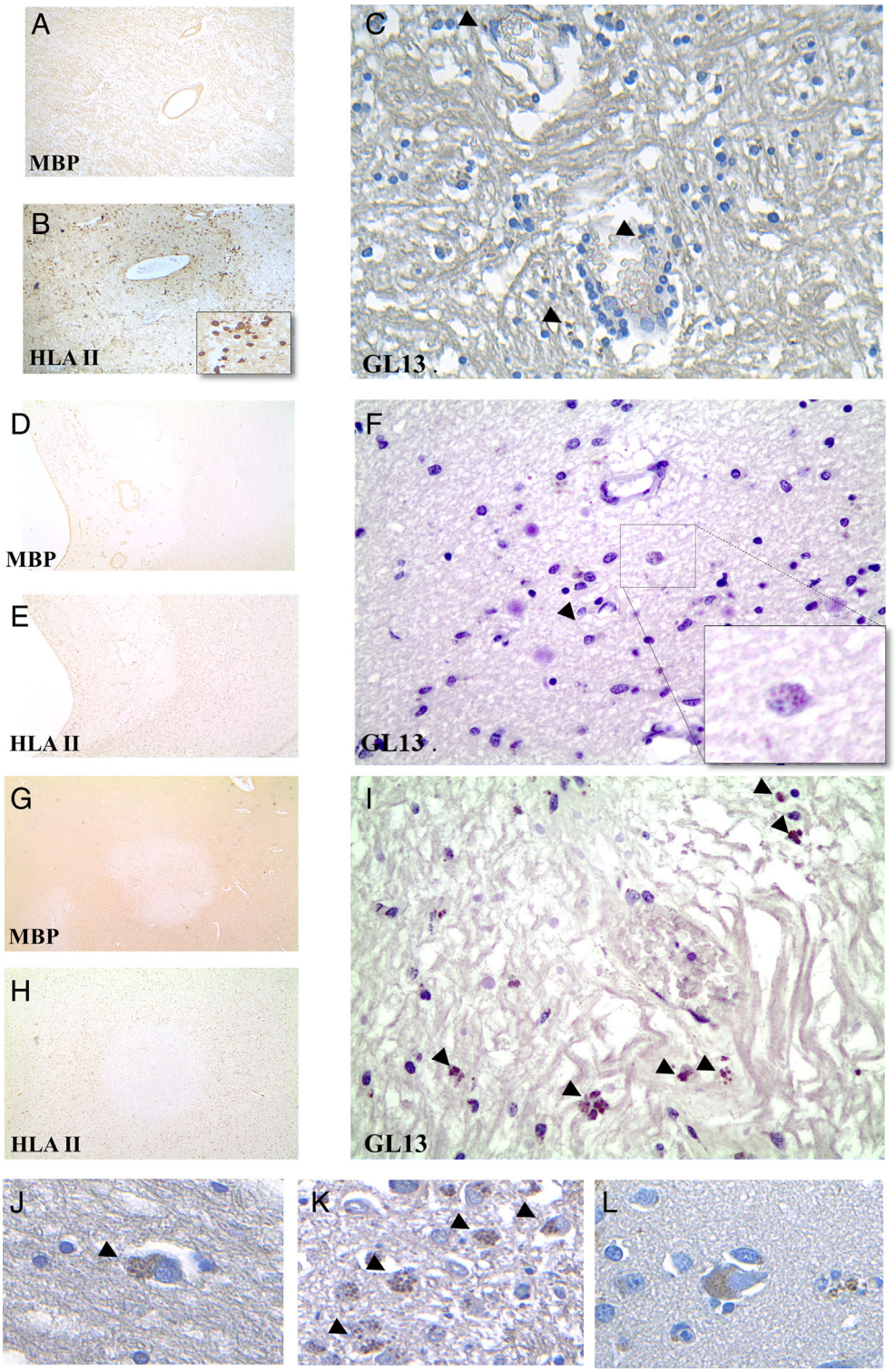

FIGURE 6: GL13 immunostaining of demyelinated lesions. MBP-stained acute active WML (A) diffusely infiltrated by HLA-II^{+} cells with macrophage morphology (*inset*) (B) exhibiting lipofuscin aggregates in glial cells and perivascular immune cells (*arrows*) (C). MBP-stained chronic active WML (D) with HLA-II^{+} cells with macrophage morphology in the lesion margins (E) exhibiting lipofuscin aggregates in glial cells (F). MBP-stained chronic inactive white matter lesion (G) infiltrated by sparse HLA-II^{+} ramified microglia (H) exhibiting lipofuscin aggregates in glial cells (I). In a greater magnification, the glial cells with lipofuscin accumulation (J), macrophages with granular GL13 staining in the actively demyelinating rim of an acute active lesion (K), and neurons with lipofuscin accumulation (L). WMLs = white matter demyelinated lesions. [Color figure can be viewed at www.annalsofneurology.org]

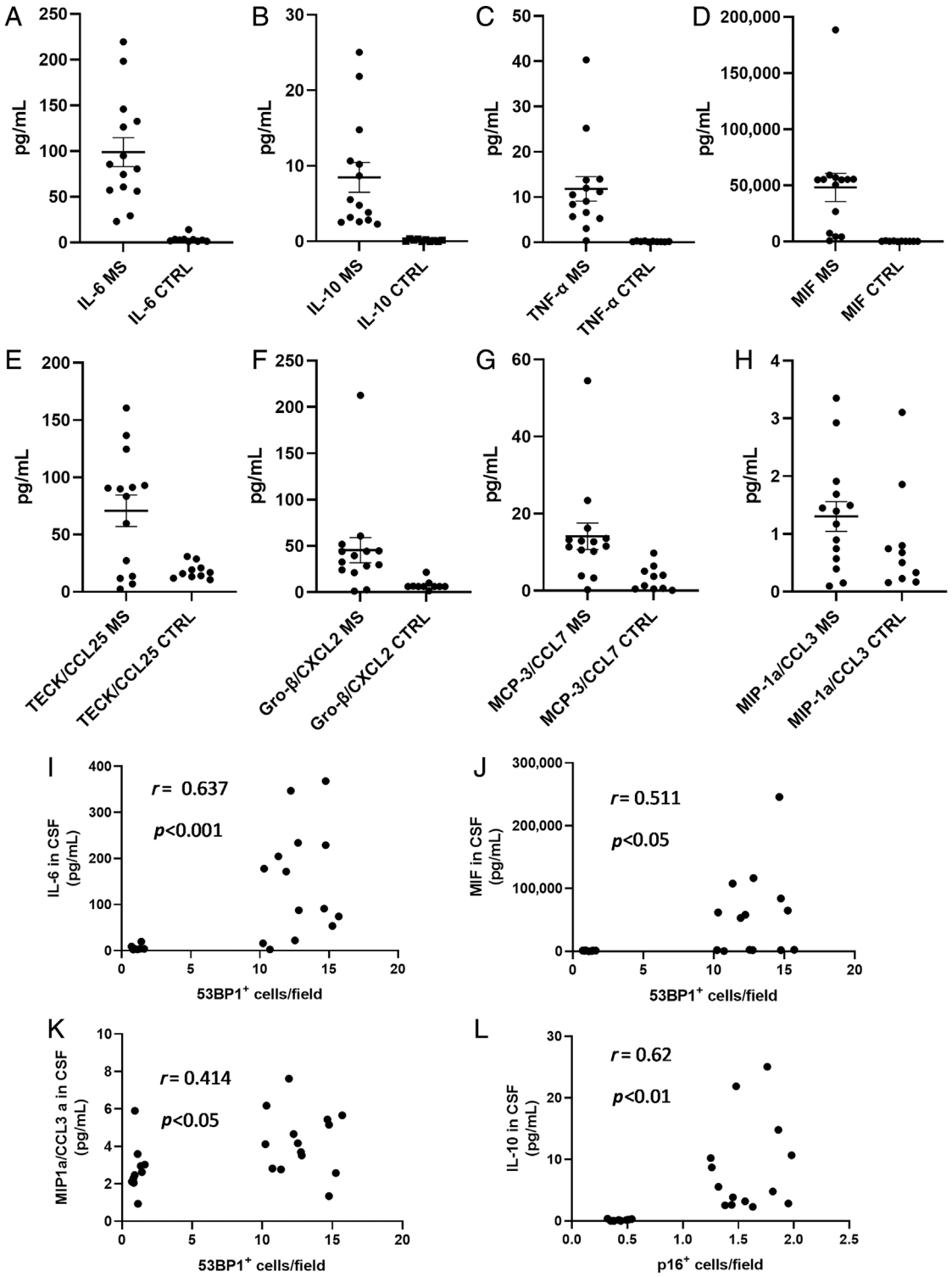

FIGURE 7: Significantly higher levels of several SASP factors were found in the CSF of patients with P-MS compared with healthy controls some of which also exhibited significant correlations with markers of cellular senescence. (A) IL-6, $p < 0.001$; (B) IL-10, $p < 0.001$; (C): TNF-α, $p < 0.01$; (D): MIF, $p < 0.05$; (E): TECK/CCL25, $p < 0.001$; (F): Gro-β/CXCL2, $p < 0.01$; (G): MCP-3/CCL7, $p < 0.01$; (H): MIP-1a/CCL3, $p < 0.05$; (I): CSF IL-6 levels exhibited a significant correlation with $53BP1^+$ cell counts in NAGM, ($r_P = 0.637$, $p < 0.001$, n = 24). (J): CSF MIF levels correlated significantly with $53BP1^+$ cell counts in NAGM ($r_P = 0.511$, $p < 0.05$, n = 24). (K): MIP1a/CCL3 levels correlated with $53BP1^+$ cell counts in NAGM, ($r_P = 0.414$, $p = 0.05$, n = 24). (L): IL-10 CSF levels exhibited a significant correlation with $p16^+$ cell counts in the NAWM ($r_P = 0.62$, $p < 0.01$, $n = 24$). Comparisons were tested with the Student's *t* test. Error bars = mean ± SEM. Correlations were tested with the Pearson's correlation coefficient. CSF = cerebrospinal fluid; NAGM = normal appearing gray matter; NAWM = normal appearing white matter; P-MS = progressive multiple sclerosis; SASP = senescence-associated secretory phenotype.

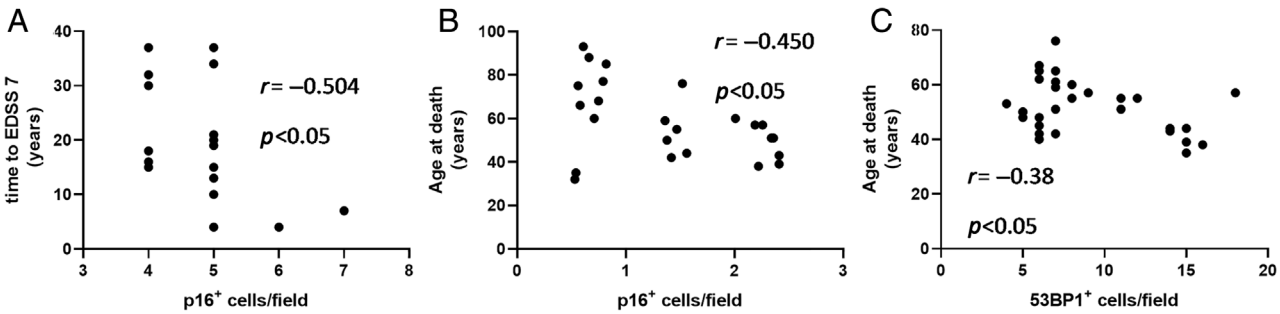

FIGURE 8: Correlations between markers of senescence and milestones of disability. (A) The p16$^+$ cell counts in WMLs exhibit a significant inverse correlation with the time from diagnosis to requiring a wheelchair (time to EDSS 7.0; $r_P = -0.504$, $p < 0.05$, $n = 17$). (B) Correlation analysis of p16$^+$ cell counts in NAGM with age at death revealed a significant inverse correlation ($r_P = -0.45$, $p < 0.05$, $n = 24$). (C) The 53BP1$^+$ cell counts exhibited an inverse correlation with age at death in WMLs ($r_P = -0.38$, $p < 0.05$, $n = 30$). Correlations were tested with the Pearson's correlation coefficient. EDSS = Expanded Disability Status Scale; NAGM = normal appearing gray matter; WML = white matter demyelinated lesion.

MS, as mouse models of mitochondrial dysfunction have been shown to exhibit increased senescence.[43] Chronic low-level inflammation has been linked to commitment to senescence in vivo[36] and cytokines, such as TGF-beta, which has been found increased in the blood of patients with MS[44] and in MS peri-plagues may also act as triggers of CS in MS.[45,46]

A causative role for CS in the etiopathogenesis of MS is unsubstantiated and counterintuitive. However, CS may substantially contribute to MS pathogenesis making an impact on the age at disease presentation and rate of worsening in the progressive forms of MS. Our finding of an association between the senescent cell load and the time to requiring a wheelchair and age at death corroborate this hypothesis. The putative detrimental effects of CS are thought to be mediated by 3 mechanisms: first, all resident cells converting to senescence acquire a pro-inflammatory phenotype and become sources of chronic parenchymal inflammation at least partly independent of the acquired and innate immune response. SASP-related inflammation may also to some extent explain the resistance of progressive MS to our immunomodulatory strategies.[7,14,25] Second, cell-cycle arrest of adult progenitor cells in the context of CS may exhaust the regenerative capacities of the nervous tissue, including its remyelinating potential.[47,48] Third, neurodegeneration in progressive MS may be driven by senescence-associated loss of neuronal and glial function, causing neuroaxonal injury as replication arrest, changes in gene expression, and other phenotypic changes that accompany cellular senescence constitute serious restrictions in the functionality of neurons and glia.[13]

Cellular senescence has been shown to affect neurons, microglia, astrocytes, oligodendrocytes, oligodendrocyte progenitor cells, pericytes, and endothelial cells under different conditions.[49–52] Sox2$^+$ progenitors from demyelinated WMLs from autopsy material and neural progenitor cells from induced pluripotent stem cell lines coming from patients with P-MS have been found to express markers of CS. These senescent progenitor cells exhibited impaired capacity to support oligodendrocyte maturation in vitro.[53] In a more recent study, in vitro exposure of fibroblasts from young individuals directly converted to oligodendrocytes to supernatants from pro-inflammatory microglia resulted in impaired differentiation and myelination as well as in upregulation of cellular senescence markers, suggesting that increased levels of pro-inflammatory cytokines secreted by microglia from patients with MS may result in accelerated aging of oligodendrocytes.[54] We have provided evidence of CS affecting neurons, astrocytes, microglia, and oligodendrocytes/oligodendrocyte progenitor cells in demyelinated and normal-appearing gray and white matter of P-MS autopsy material. As the markers used are indicative of DDR, cell-cycle arrest, and metabolic derangement, which are features of CS but are not entirely specific for CS, the exact number of senescent cells in WMLs and GMLs could not be quantified.[12] Our tentative estimate based on the double p16$^+$/GL13$^+$ staining would be that senescent cells should not exceed 18 and 9% of cells in acute active WMLs and GMLs, respectively.

As SASP is thought to partly mediate the detrimental actions of senescent cells, we examined several key SASP factors in our samples. Macrophage migration inhibitory factor (MIF) is a common SASP mediator expressed by macrophages capable of promoting inflammatory responses by enhancing NF-κB signaling and repressing the function of p53.[55,56] MIF was found significantly increased in the CSF of our P-MS cases compared with healthy controls and its levels correlated with the number of cells with activated DDR (53BP1$^+$ cells) in NAGM. MIP1a/CCL3 is another SASP factor whose levels correlated with the extent of DDR activation in NAGM. MIP1a/CCL3 is known to be upregulated in the

CSF of patients with MS and its levels are linked to a poorer prognosis.[57] Interleukin-6 is another pleiotropic pro-inflammatory cytokine[58] produced by astrocytes and microglia, which has been reported increased in the CSF across all MS phenotypes.[59] Our data link this increase in IL-6 to the extent of DDR activation in NAGM.

We have demonstrated that senescent cells are greatly more abundant in acute active white and gray matter lesions compared with chronic inactive ones, which suggests that, along with the evolution of the lesion, senescent cells are at least partly somehow being removed. There is compelling evidence for an interaction between senescent cells and the immune system. Senescent cells have been shown to attract macrophages and natural killer (NK) cells with their SASP pro-inflammatory mediators.[20,21,60] NK cells may kill senescent cells with perforin and granzyme-containing granule exocytosis and may also promote macrophage-mediated phagocytosis by producing IFN-γ.[60] In addition, T helper lymphocytes have been found to directly recognize senescent cells.[18] Senescent cell clearance by the immune system is thought to be highly regulated and may contribute to the accelerated brain volume loss seen in MS.[61–63]

Recognizing CS as a pathogenetic mechanism of age-related neurodegeneration could provide a promising therapeutic target for neuroprotection, aiming at preventing disability progression in P-MS. In vitro and in vivo studies of agents aiming to promote the selective death of senescent cells (senolysis) or to block the damaging effects of the SASP-related mediators (senomorphism) have so far yielded encouraging results.[64] In the PS19 transgenic model of tau-dependent neurodegeneration, treatment with the senolytic compound ABT263 reduced tau phosphorylation and aggregation and improved memory deficits by removing senescent glial cells.[23] Furthermore, rapamycin treatment of neural progenitor cells produced from induced pluripotent stem cells from patients with progressive MS modified their senescent state and improved their capacity to promote oligodendrocyte progenitor cell differentiation in vitro, providing evidence that senomorphic treatment may enhance remyelination.[53] Simvastatin, which has shown efficacy in preventing disability progression and brain atrophy in P-MS[65] may downregulate p38MAPK activation and SASP markers TNFa, and GM-CSF suggesting that its neuroprotective effects may be mediated by its senomorphic actions.[66] Reprogramming senescent cells or enhancing their immune-mediated physiological clearance may constitute another senotherapeutic approach.[64] Senotherapy in MS could aim at preventing senescence-associated SASP factor-mediated chronic inflammation, loss of cell function, and neuroaxonal loss and promoting remyelination.

Nevertheless, our study does not provide direct evidence of a pathogenetic role of CS in driving disability progression in MS. The complex physiological and pathophysiological roles of CS, along with the cell-specificity of senescence triggers and phenotypes, necessitates a thorough investigation of the biology of CS of neurons and glial cells, its eliciting factors, and mediators. Defining the senescent secretome of neurons and glial cells in progressive MS could help to elucidate the exact contribution of each cell type to disability progression and to identify senescence-based molecular signatures as many inflammatory mediators are not truly unique to senescent cells. The definition of molecular signatures of senescence may also pave the way for the development of senescence-related biomarkers of progression.

In conclusion, our data provides evidence of accelerated cellular senescence in progressive MS. We demonstrated CS being most extensive in actively demyelinating gray and white matter lesions but also present in chronic inactive lesions and normal appearing gray and white matter and affecting both neurons and all glial cell types. Our data corroborate the hypothesis of cellular senescence playing a detrimental role in progressive MS. Nevertheless, these findings merit further investigation to elucidate the exact mechanisms and the senescent cell types involved in promoting age-related neurodegeneration in P-MS. If the pathogenetic role of CS in driving neurodegeneration and disability progression in MS is confirmed, senotherapic approaches may prove to be the game-changing neuroprotective strategies to prevent and potentially reverse progressive disability in MS.

Acknowledgments

The authors are indebted to the staff of the MS and PD tissue banks at Imperial College, Hammersmith Hospital for their invaluable assistance in the provision of tissues and related demographic data. We are also grateful to Ms Myrto Papadopoulou for her assistance in image editing and formatting. This work was funded by a research grant from the UK Multiple Sclerosis Society.

Author Contributions

D.P., R.M., R.R., and R.N. contributed to the conception and design of the study. S.B., I.C., E.B., and D.P. contributed to the acquisition and analysis of data. D.P., L.P., V.G., R.R., and R.N. contributed to drafting and revision of the manuscript.

Potential Conflicts of Interest

The authors have no conflicts of interest to report.

Data Availability

All data remain available at the Department of Neurosciences and Biomedicine and Movement of the University Hospital of Verona, Italy and the Department of Brain Sciences, Faculty of Medicine, Imperial College London, UK, upon request to the corresponding author.

References

1. Scalfari A, Neuhaus A, Daumer M, et al. Age and disability accumulation in multiple sclerosis. Neurology 2011;77:1246–1252.
2. Harding KE, Liang K, Cossburn MD, et al. Long-term outcome of paediatric-onset multiple sclerosis: a population-based study. J Neurol Neurosurg Psychiatry 2013;84:141–147.
3. Stankoff B, Mrejen S, Tourbah A, et al. Age at onset determines the occurrence of the progressive phase of multiple sclerosis. Neurology 2007;68:779–781.
4. Trapp BD, Nave KA. Multiple sclerosis: an immune or neurodegenerative disorder? Annu Rev Neurosci 2008;31:247–269.
5. Graves JS, Krysko KM, Hua LH, et al. Ageing and multiple sclerosis. Lancet Neurol 2023;22:66–77.
6. Martínez-Cué C, Rueda N. Cellular senescence in neurodegenerative diseases. Front Cell Neurosci 2020;14:16.
7. Oost W, Talma N, Meilof JF, Laman JD. Targeting senescence to delay progression of multiple sclerosis. J Mol Med (Berl) 2018;96:1153–1166. https://doi.org/10.1007/s00109-018-1686-x.
8. Howcroft TK, Campisi J, Louis GB, et al. The role of inflammation in age-related disease. Aging (Albany NY) 2013;5:84–93.
9. López-Otín C, Blasco MA, Partridge L, et al. The hallmarks of aging. Cell 2013;153:1194–1217.
10. Mahad D, Ziabreva I, Lassmann H, Turnbull D. Mitochondrial defects in acute multiple sclerosis lesions. Brain 2008;131:1722–1735.
11. Hayflick L, Moorhead PS. The serial cultivation of human diploid cell strains. Exp Cell Res 1961;25:585–621.
12. Gorgoulis V, Adams PD, Alimonti A, et al. Cellular senescence: defining a path forward. Cell 2019;179:813–827.
13. Purcell M, Kruger A, Tainsky MA. Gene expression profiling of replicative and induced senescence. Cell Cycle 2014;13:3927–3937.
14. Kritsilis M, Rizou VS, Koutsoudaki PN, et al. Ageing, cellular senescence and neurodegenerative disease. Int J Mol Sci 2018;19:2937.
15. Jurk D, Wang C, Miwa S, et al. Postmitotic neurons develop a p21-dependent senescence-like phenotype driven by a DNA damage response. Aging Cell 2012;11:996–1004.
16. Herrup K, Yang Y. Cell cycle regulation in the postmitotic neuron: oxymoron or new biology? Nat Rev Neurosci 2007;8:368–378.
17. Wengerodt D, Schmeer C, Witte OW, Kretz A. Amitosenescence and Pseudomitosenescence: putative new players in the aging process. Cells 2019;8:1546.
18. Acosta JC, Banito A, Wuestefeld T, et al. A complex secretory program orchestrated by the inflammasome controls paracrine senescence. Nat Cell Biol 2013;15:978–990.
19. Chen H, Ruiz PD, McKimpson WM, et al. MacroH2A1 and ATM play opposing roles in paracrine senescence and the senescence-associated secretory phenotype. Mol Cell 2015;59:719–731.
20. Hoenicke L, Zender L. Immune surveillance of senescent cells--biological significance in cancer- and non-cancer pathologies. Carcinogenesis 2012;33:1123–1126.
21. Muñoz-Espín D, Serrano M. Cellular senescence: from physiology to pathology. Nat Rev Mol Cell Biol 2014;15:482–496.
22. Baker DJ, Petersen RC. Cellular senescence in brain aging and neurodegenerative diseases: evidence and perspectives. J Clin Invest 2018;128:1208–1216.
23. Bussian TJ, Aziz A, Meyer CF, et al. Clearance of senescent glial cells prevents tau-dependent pathology and cognitive decline. Nature 2018;562:578–582.
24. Zhang P, Kishimoto Y, Grammatikakis I, et al. Senolytic therapy alleviates Aβ-associated oligodendrocyte progenitor cell senescence and cognitive deficits in an Alzheimer's disease model. Nat Neurosci 2019;22:719–728.
25. Papadopoulos D, Magliozzi R, Mitsikostas DD, et al. Aging, cellular senescence, and progressive multiple sclerosis. Front Cell Neurosci 2020;14:178.
26. Evangelou K, Lougiakis N, Rizou SV, et al. Robust, universal biomarker assay to detect senescent cells in biological specimens. Aging Cell 2017;16:192–197.
27. Magliozzi R, Howell OW, Reeves C, et al. A gradient of neuronal loss and meningeal inflammation in multiple sclerosis. Ann Neurol 2010;68:477–493.
28. Trapp BD, Peterson J, Ransohoff RM, et al. Axonal transection in the lesions of multiple sclerosis. N Engl J Med 1998;338:278–285. https://doi.org/10.1056/NEJM199801293380502.
29. Peterson JW, Bö L, Mörk S, et al. Transected neurites, apoptotic neurons, and reduced inflammation in cortical multiple sclerosis lesions. Ann Neurol 2001;50:389–400.
30. Coppé JP, Desprez PY, Krtolica A, Campisi J. The senescence-associated secretory phenotype: the dark side of tumor suppression. Annu Rev Pathol 2010;5:99–118.
31. Kuilman T, Peeper DS. Senescence-messaging secretome: SMS-ing cellular stress. Nat Rev Cancer 2009;9:81–94.
32. Magliozzi R, Howell OW, Nicholas R, et al. Inflammatory intrathecal profiles and cortical damage in multiple sclerosis. Ann Neurol 2018;83:739–755.
33. Burd CE, Sorrentino JA, Clark KS, et al. Monitoring tumorigenesis and senescence in vivo with a p16(INK4a)-luciferase model. Cell 2013;152:340–351.
34. Howell OW, Reeves CA, Nicholas R, et al. Meningeal inflammation is widespread and linked to cortical pathology in multiple sclerosis. Brain 2011;134:2755–2771.
35. Schultz LB, Chehab NH, Malikzay A, Halazonetis TD. p53 binding protein 1 (53BP1) is an early participant in the cellular response to DNA double-strand breaks. J Cell Biol 2000;151:1381–1390. https://doi.org/10.1083/jcb.151.7.1381.
36. López-Otín C, Blasco MA, Partridge L, et al. Hallmarks of aging: an expanding universe. Cell 2023;186:243–278.
37. Haider L, Fischer MT, Frischer JM, et al. Oxidative damage in multiple sclerosis lesions. Brain 2011;134:1914–1924. https://doi.org/10.1093/brain/awr128.
38. Smith KJ, Kapoor R, Felts PA. Demyelination: the role of reactive oxygen and nitrogen species. Brain Pathol 1999;9:69–92.
39. Vladimirova O, O'Connor J, Cahill A, et al. Oxidative damage to DNA in plaques of MS brains. Mult Scler 1998;4:413–418.
40. Calvi A, Haider L, Prados F, et al. In vivo imaging of chronic active lesions in multiple sclerosis. Mult Scler 2022;28:683–690.
41. Popescu BF, Frischer JM, Webb SM, et al. Pathogenic implications of distinct patterns of iron and zinc in chronic MS lesions. Acta Neuropathol 2017;134:45–64.
42. Campbell GR, Ziabreva I, Reeve AK, et al. Mitochondrial DNA deletions and neurodegeneration in multiple sclerosis. Ann Neurol 2011;69:481–492.

43. Wiley CD, Velarde MC, Lecot P, et al. Mitochondrial dysfunction induces senescence with a distinct secretory phenotype. Cell Metab 2016;23:303–314.

44. Flauzino T, Alfieri DF, de Carvalho Jennings Pereira WL, et al. The rs3761548 FOXP3 variant is associated with multiple sclerosis and transforming growth factor β1 levels in female patients. Inflamm Res 2019;68:933–943.

45. Nataf S, Guillen M, Pays L. Irrespective of plaque activity, multiple sclerosis brain Periplaques exhibit alterations of myelin genes and a TGF-Beta signature. Int J Mol Sci 2022;23:14993.

46. Preininger MK, Zaytseva D, Lin JM, Kaufer D. Blood-brain barrier dysfunction promotes astrocyte senescence through albumin-induced TGFβ signaling activation. Aging Cell 2023;5:e13747.

47. Koutsoudaki PN, Papadopoulos D, Passias PG, et al. Cellular senescence and failure of myelin repair in multiple sclerosis. Mech Ageing Dev 2020;192:111366.

48. Patani R, Balaratnam M, Vora A, Reynolds R. Remyelination can be extensive in multiple sclerosis despite a long disease course. Neuropathol Appl Neurobiol 2007;33:277–287.

49. Bhat R, Crowe EP, Bitto A, et al. Astrocyte senescence as a component of Alzheimer's disease. PLoS One 2012;7:e45069.

50. Kiss T, Nyúl-Tóth Á, Balasubramanian P, et al. Single-cell RNA sequencing identifies senescent cerebromicrovascular endothelial cells in the aged mouse brain. Geroscience 2020;42:429–444.

51. Yamazaki Y, Baker DJ, Tachibana M, et al. Vascular cell senescence contributes to blood-brain barrier breakdown. Stroke 2016;47:1068–1077.

52. Kujuro Y, Suzuki N, Kondo T. Esophageal cancer-related gene 4 is a secreted inducer of cell senescence expressed by aged CNS precursor cells. Proc Natl Acad Sci U S A 2010;107:8259–8264.

53. Nicaise AM, Wagstaff LJ, Willis CM, et al. Cellular senescence in progenitor cells contributes to diminished remyelination potential in progressive multiple sclerosis. Proc Natl Acad Sci U S A 2019;116:9030–9039.

54. Windener F, Grewing L, Thomas C, et al. Physiological aging and inflammation-induced cellular senescence may contribute to oligodendroglial dysfunction in MS. Acta Neuropathol 2024;147:82.

55. Calandra T, Bernhagen J, Mitchell RA, Bucala R. The macrophage is an important and previously unrecognized source of macrophage migration inhibitory factor. J Exp Med 1994;179:1895–1902.

56. Salminen A, Kaarniranta K. Control of p53 and NF-κB signaling by WIP1 and MIF: role in cellular senescence and organismal aging. Cell Signal 2011;23:747–752.

57. Puthenparampil M, Stropparo E, Zywicki S, et al. Wide cytokine analysis in cerebrospinal fluid at diagnosis identified CCL-3 as a possible prognostic factor for multiple sclerosis. Front Immunol 2020;11:174.

58. Rothaug M, Becker-Pauly C, Rose-John S. The role of interleukin-6 signaling in nervous tissue. Biochim Biophys Acta 2016;1863:1218–1227.

59. Stampanoni Bassi M, Iezzi E, Drulovic J, et al. IL-6 in the cerebrospinal fluid signals disease activity in multiple sclerosis. Front Cell Neurosci 2020;14:120.

60. Antonangeli F, Zingoni A, Soriani A, Santoni A. Senescent cells: living or dying is a matter of NK cells. J Leukoc Biol 2019;105:1275–1283.

61. Xue W, Zender L, Miething C, et al. Senescence and tumour clearance is triggered by p53 restoration in murine liver carcinomas. Nature 2007;445:656–660.

62. De Stefano N, Stromillo ML, Giorgio A, et al. Establishing pathological cut-offs of brain atrophy rates in multiple sclerosis. J Neurol Neurosurg Psychiatry 2016;87:93–99.

63. Ovadya Y, Landsberger T, Leins H, et al. Impaired immune surveillance accelerates accumulation of senescent cells and aging. Nat Commun 2018;9:5435.

64. Thoppil H, Riabowol K. Senolytics: a translational bridge between cellular senescence and organismal aging. Front Cell Dev Biol 2020;7:367.

65. Chataway J, Schuerer N, Alsanousi A, et al. Effect of high-dose simvastatin on brain atrophy and disability in secondary progressive multiple sclerosis (MS-STAT): a randomised, placebo-controlled, phase 2 trial. Lancet 2014;383:2213–2221. https://doi.org/10.1016/S0140-6736(13)62242-4.

66. Ayad MT, Taylor BD, Menon R. Regulation of p38 mitogen-activated kinase-mediated fetal membrane senescence by statins. Am J Reprod Immunol 2018;80:e12999. https://doi.org/10.1111/aji.12999.